Supplementary Information

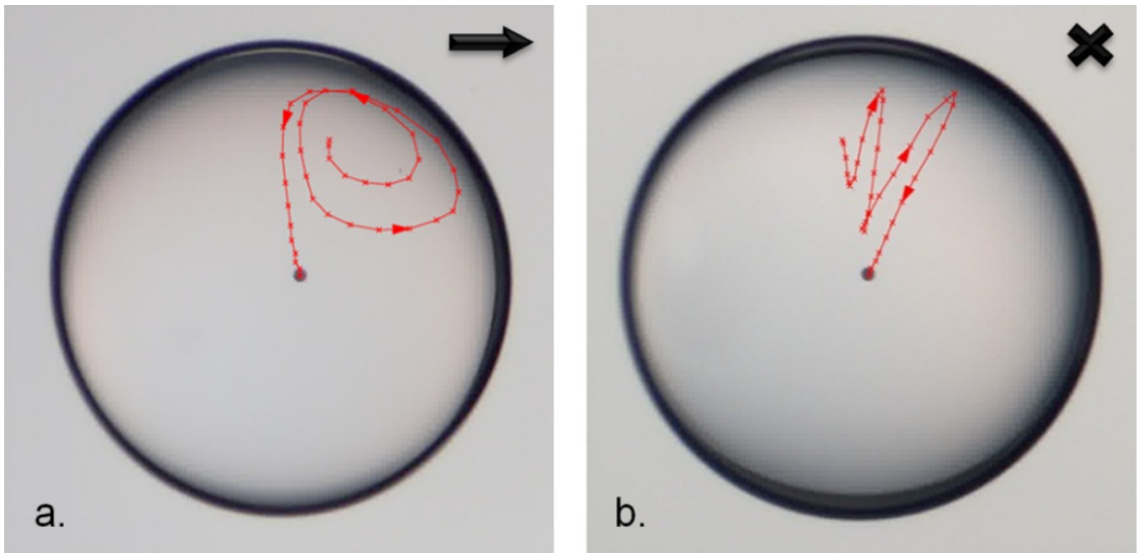

Supplementary Figure S1. Tracing of a particle inside a drop. Silicone drop of radius about 1 mm at E=160 Vmm^{-1} with PE bead used to trace the flow inside the drop. Drop imaged perpendicular (**a**) and parallel (**b**) to the direction of **E**-field. It is seen that the particle follows a spiral motion, i.e. changing between the closed Taylor loop paths as it approaches the drop surface.

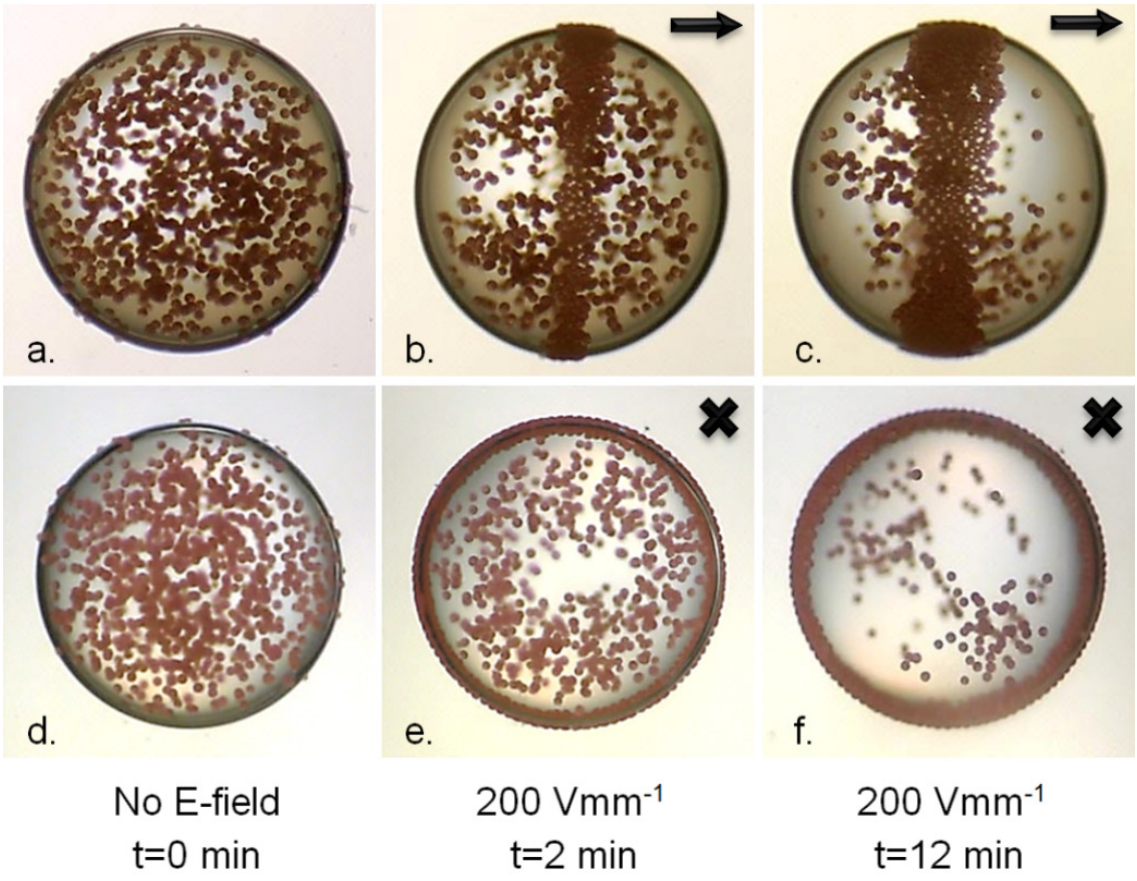

Supplementary Figure S2. Assembly of colloidal polyethylene surface ribbon. A silicone oil drop of radius around 0.75 mm with polyethylene (PE) particles initially dispersed throughout the drop. The drop is immersed in castor oil. The arrows and crosses indicate the direction of the **E**-field. The three upper panels (**a,b,c**) are viewed perpendicular to the **E**-field direction, while the three lower panels (**d,e,f**) are viewed along the **E**-field direction. (**a**) and (**d**) show the situation before the **E**-field is turned on, and (**b,c**) and (**e,f**) after a DC electric field is applied. Hydrodynamic circulation flows are observed in the drop, and after a few minutes a ribbon shaped colloidal monolayer is assembled on the drop surface. A significant number of particles are still carried by the flow in the bulk of the drop. The drop has an oblate deformation.

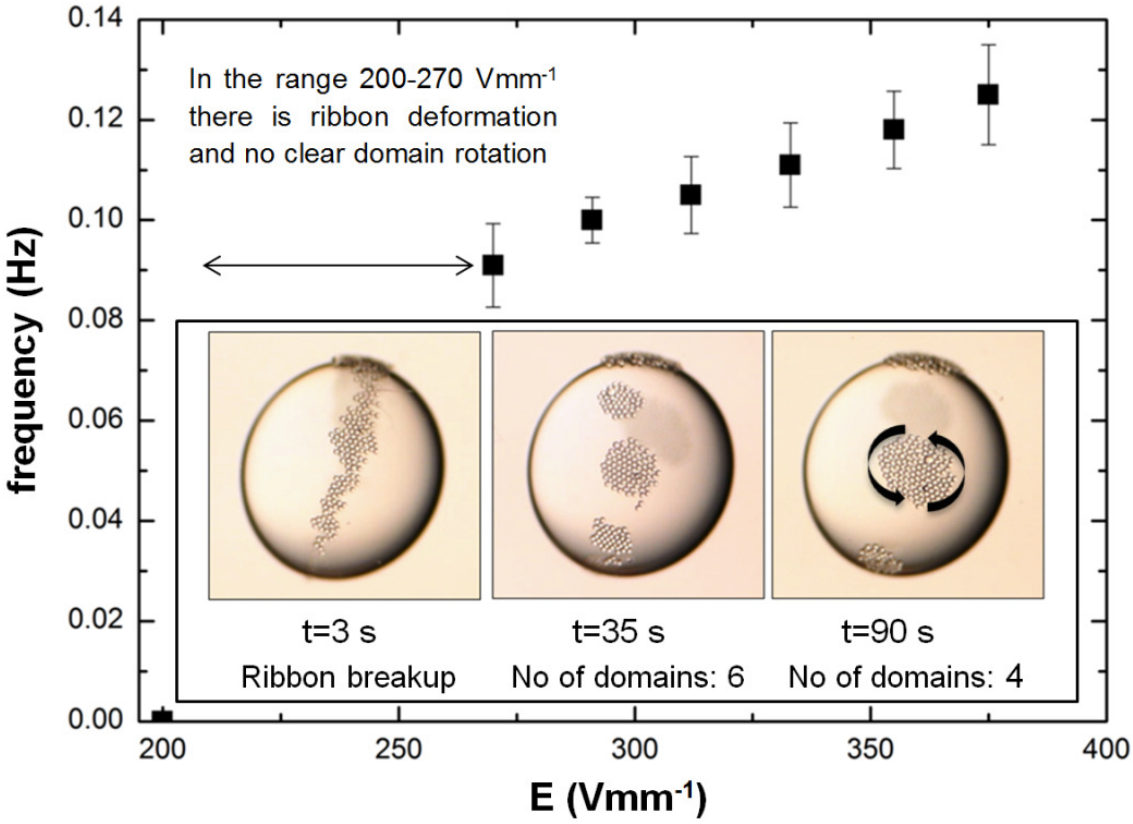

Supplementary Figure S3. **Domain rotation frequency versus electric field strength**. At 300 V/mm the rotation frequency is of order of magnitude 0.1 Hz and increases with electric field with a rate of approximately 4×10^{-4} $mmV^{-1}s^{-1}$ (within the range of 275 to 375 Vmm^{-1}). In the range 200 to 270 Vmm^{-1} there is ribbon deformation and the domains are not clearly defined. At even lower fields, i.e. below 200 Vmm^{-1} the ribbon is static. The inset pictures show an example of a droplet with radius about 1 mm with rotating domain structures at different times after the electric field is suddenly increased from 0 to 375 Vmm^{-1} at time t=0. The **E**-field direction is horizontal in the plane of the panels, as indicated by the arrows. This is illustrated in more detail in the Supplementary Movie 3.

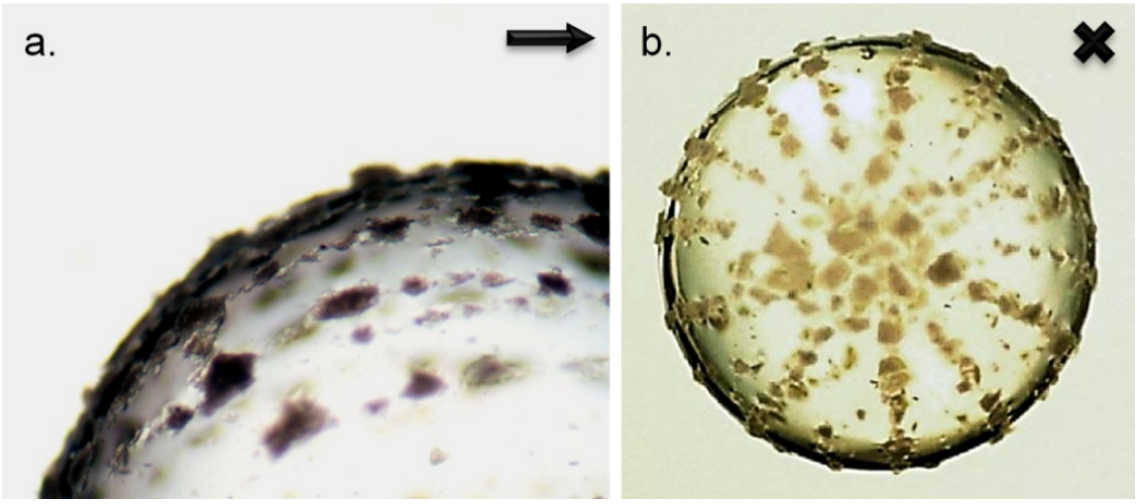

Supplementary Figure S4. Colloidal cage formed by large fluorohectorite clay platelet particles. (**a**) Detail of clay chains on drop surface. (**b**) Clay chain structures seen in the direction of the electric field. The drop radius is about 1 mm and the electric field strength is 250 Vmm^{-1}.

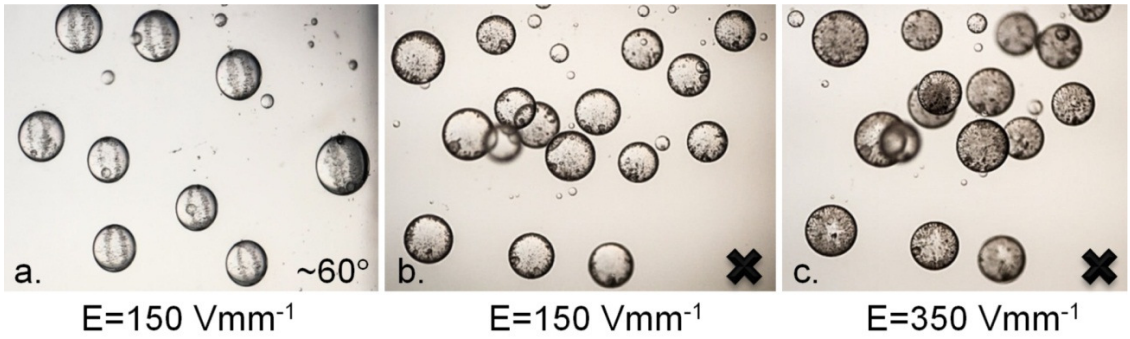

Supplementary Figure S5. Active structuring of colloidal armour on multiple drops. (**a**) Simultaneously formed ribbons of fluorohectorite clay particles at the surface of several silicone oil drops (viewed at an angle ~60° with respect to the direction of electric field). Simultaneous opening (**b**) and closing (**c**) of pupils for multiple drops. The drop radii are in the range of 0.6 to 0.8 mm.

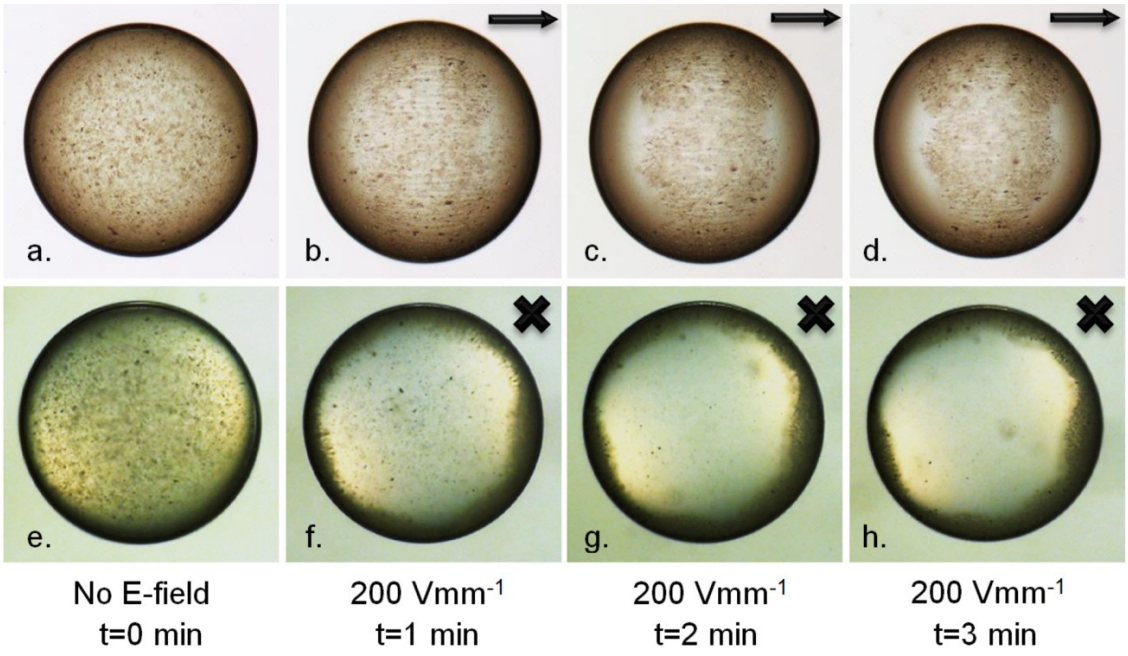

Supplementary Figure S6. Assembly of colloidal clay surface ribbon at at *E*=200 Vmm^{-1}. A silicone oil drop radius of 0.7 mm with fluorohectorite clay particles initially dispersed throughout the drop. The drop is immersed in castor oil. The arrows and crosses indicate the direction of the **E**-field. The four upper panels (**a,b,c,d**) are viewed perpendicular to the **E**-field direction, while the four lower panels (**e,f,g,h**) are viewed along the **E**-field direction. (**a**) and (**e**) show the situation before the **E**-field is turned on, and (**b,c,d**) and (**f,g,h**) after a DC electric field is applied.

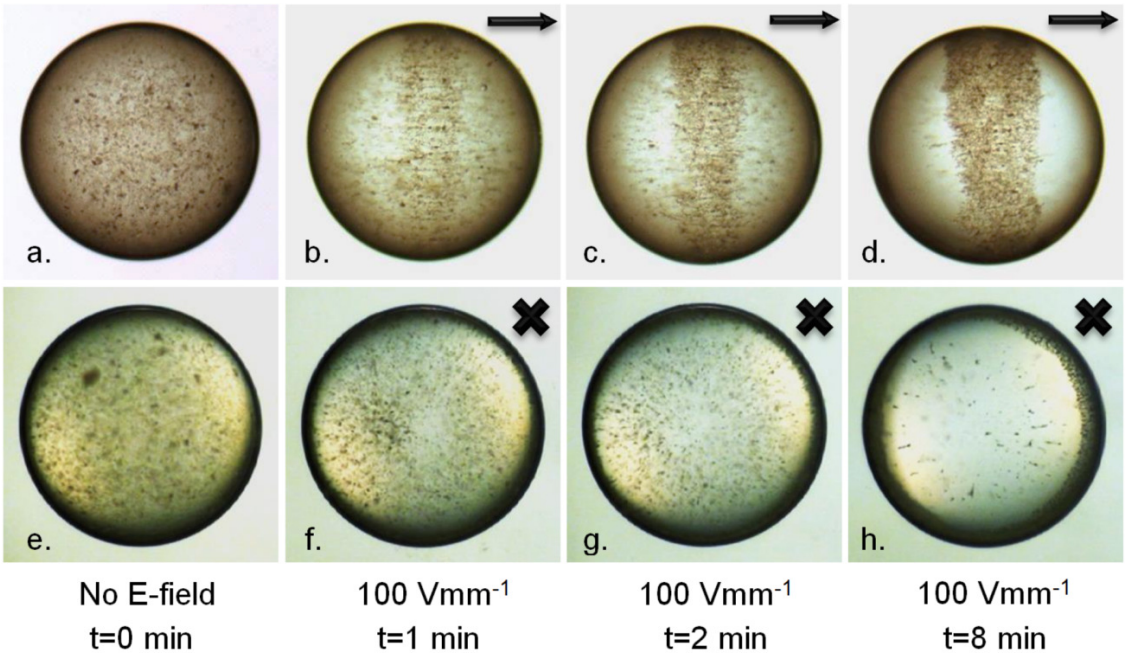

Supplementary Figure S7. Assembly of colloidal clay surface ribbon at E=100 Vmm^{-1}. The panel description is identical to the description in Supplementary Figure S6. In this case however, the time scale of the ribbon formation is significantly slower due to the lower electric field strength.

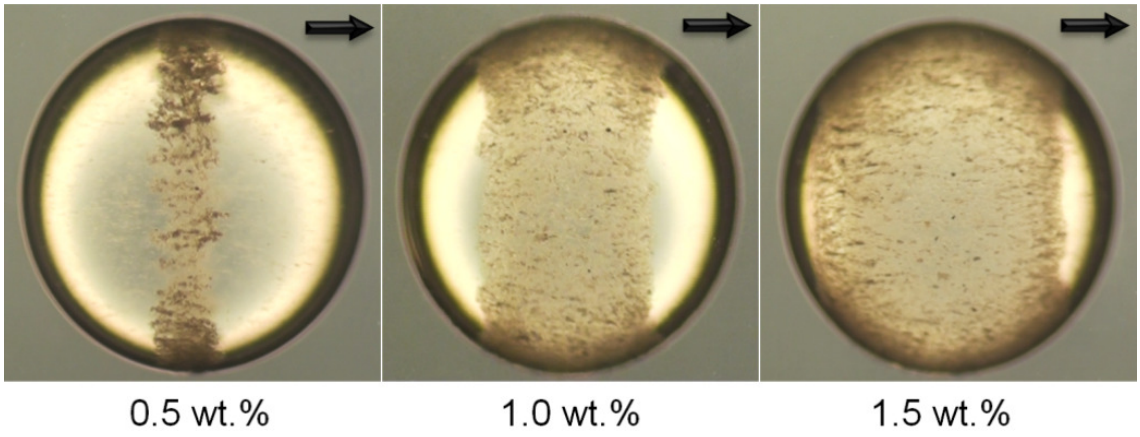

Supplementary Figure S8. Ribbon width as a function of clay concentration. For higher colloidal concentration, the ribbon becomes wider. The drop radius is about 1 mm. The **E**-field direction is horizontal in the plane of the panels, as indicated by the arrows.

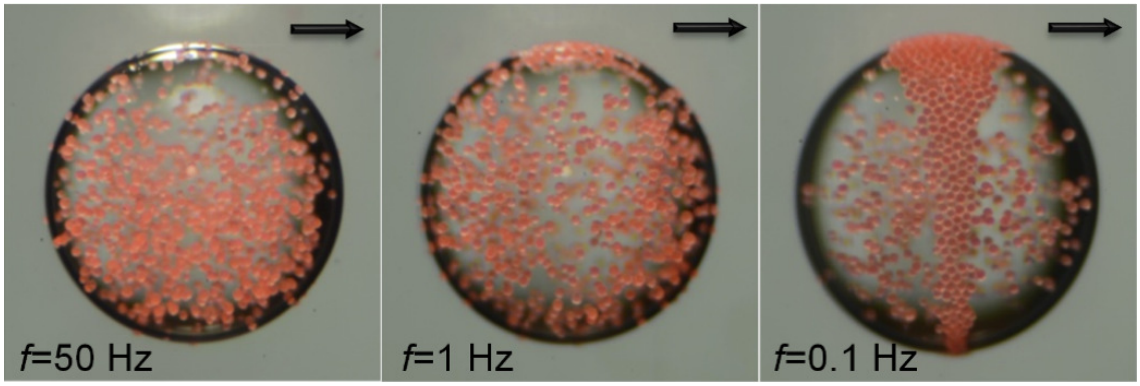

Supplementary Figure S9. Ribbon formation of PE beads at various AC field frequencies. Silicone drop of radius about 0.5 mm with PE beads in AC field at different frequencies, *f*. The **E**-field direction is horizontal in the plane of the panels, as indicated by the arrows.

Supplementary Table S1. **Pupil formation related to electrical conductivity.** The relative electrical conductivities of different clay powders are normalized to that of Kaolinite (~2×10^{-6} Sm^{-1}). Only clay minerals with high conductivity values display active pupil-like formation.

Clay mineral	Kaolinite	Quick clay	Halloysite	Vermiculite	Na-MMT	Fe-Fh	Cu-Fh	Li-Fh	Laponite
Relative conductivity	1.0	1.2 ± 16 %	1.9 ± 21 %	2.7 ± 33 %	3.0 ± 27 %	12.6 ± 17 %	17.0 ± 24 %	42.6 ± 26 %	89.6 ± 28 %
Pupil formation	No	No	No	No	No	Yes	Yes	Yes	Yes